



OPEN

Metabolite profiling of Arabidopsis mutants of lower glycolysis

DATA DESCRIPTOR

Youjun Zhang ^{1,2} & Alisdair R. Fernie^{1,2}

We have previously shown that in Arabidopsis the three enzymes of lower glycolysis namely phosphoglycerate mutase (PGAM), enolase and pyruvate kinase form a complex which plays an important role in tethering the mitochondria to the chloroplast. Given that the metabolism of these mutants, the complemented of *pgam* mutant and overexpression lines of PGAM were unclear, here, we present gas chromatography mass spectrometry-based metabolomics data of them alongside their plant growth phenotypes. Compared with wild type, both sugar and amino acid concentration are significantly altered in *phosphoglycerate mutase*, *enolase* and *pyruvate kinase*. Conversely, overexpression of PGAM could decrease the content of 3PGA, sugar and several amino acids and increase the content of alanine and pyruvate. In addition, the *pgam* mutant could not be fully complemented by either a nuclear target *pgam*, a side-directed-mutate of *pgam* or a the *E. coli* PGAM in term of plant phenotype or metabolite profiles, suggesting the low glycolysis complete formation is required to support normal metabolism and growth.

Background & Summary

As one of the hallmark pathways of respiration, glycolysis provides carbon skeletons for the biosynthesis of a wide range of metabolites as well as being at the heart of energy transformations^{1,2}. In plants, enzymes of glycolysis exist both in the cytosol and plastid, and thus parallel reactions are catalyzed by differentially localized nuclear-encoded isoenzymes. In plant two ATP-independent network containing alternate cytosolic reactions enhance the pathway's ATP yield via utilizing pyrophosphate in place of ATP. In the dark, starch is degraded to glucose, and then provides the energy and carbon skeletons by cytosol glycolytic pathway and mitochondrial TCA cycle for the plant growth and development³. Chloroplasts and non-photosynthetic plastids use an incomplete glycolytic pathway to breakdown starch as well as to generate carbon skeletons, reductant, and ATP for anabolic pathways such as fatty acid synthesis^{1,3}. In the light, 3-phosphoglyceric acid (3PGA) and Glyceraldehyde 3-phosphate (GAP) are produced by photosynthesis and used to synthesize the RuBP and starch in the chloroplast generating ATP either via photophosphorylation or by oxidative phosphorylation to provide energy for metabolic reactions. It has long been reported that GAP and 3PGA are exported to the cytosol by the triose phosphate translocator⁴. This 3PGA could subsequently be converted to pyruvate where after it can be incorporated into the TCA cycle, while GAP could be used to synthesize sucrose or alternative be converted to pyruvate to supply into the TCA cycle^{5,6}. In addition, the rate of plant glycolytic flux mostly adjusts to energy and the carbon skeleton demand.

In lower cytosolic glycolysis, phosphoglycerate kinase (PGK) is involved in both photosynthetic carbon metabolism and glycolysis/gluconeogenesis⁷. Phosphoglycerate kinase (PGK) could catalyze the reversible reaction transferring a phosphate group from 1,3-bisphosphoglycerate (1,3-BPG) to ADP producing 3PGA and ATP¹. Indeed, the cytosolic *pgk* knockout mutant was characterized as having reduced growth but higher starch levels than the wild type⁷. In addition, the single phosphate group left on the 3PGA could be transferred to central carbon by 2,3-bisphosphoglycerate-independent phosphoglycerate mutase (PGAM) to produce 2-phosphoglycerate (2-PGA). Although single *pgam* mutants were similar to the wild type in all plant phenotypes assayed, double mutants had no detectable PGAM activity and showed defects in abscisic acid-, blue light-, and low CO₂-regulated stomatal movement⁸. Vegetative plant growth was also severely impaired in the double mutants and no pollen was produced⁸. The subsequent step of the pathway that is catalyzed by enolases result in the reversible dehydration of 2-PGA to phosphoenolpyruvate (PEP) which is required for both ATP production and aromatic compound and secondary metabolite biosynthesis⁹. Interestingly, cytosolic enolase encodes

¹Center of Plant Systems Biology and Biotechnology, 4000, Plovdiv, Bulgaria. ²Max-Planck-Institut für Molekulare Pflanzenphysiologie, Am Mühlenberg 1, 14476, Potsdam-Golm, Germany. e-mail: yozhang@mpimp-golm.mpg.de; fernie@mpimp-golm.mpg.de

two proteins namely a full-length enolase and a truncated version cMyc binding protein (AtMBP-1) which is a nuclear localized transcript factor¹⁰. The single *enolase* mutant displays several cellular defects including reduced cell size, defective cell differentiation with restricted lignification, as well as, altered vascular development, impaired floral organogenesis and defective male gametophyte function, resulting in embryo lethality⁹. The last enzyme of the glycolysis is pyruvate kinase which is important not only in ATP production but also in providing carbon skeleton for fatty acid biosynthesis. In *Arabidopsis*, five identified cytosolic pyruvate kinase isoforms adjust the carbohydrate flux through the glycolytic pathway¹¹. Both PKC3 and PKC4 are dual localized to the cytosol and mitochondrial outer membrane but mutants of all isoforms have not yet been studied. Although the plant growth phenotype and physiology of the remaining lower glycolytic mutants were well investigated, the metabolic consequences of these genetic interventions, with the exception of the *pgk* mutant, have not been well characterized.

In our previous research, the glycolytic complex of PGAM, enolase and pyruvate kinase was found to not only be involved in substrate channeling but also have a moonlighting role in mediating the co-localization of mitochondria and chloroplasts². Two studies suggested that PGAM and enolase are formed a metabolon which efficiently converts 3PGA to 2PGA at the outer membrane of the mitochondria. Given that the double mutant of the *pgam* displayed greatly inhibited growth, it is important to understand the metabolic function of the metabolon by complementing *pgam* mutants using *E.coli* homologs, as well as non-functional and nuclear targeted PGAMs. In addition, given that the overexpression of the PGAM1 resulted in slightly increase in plant growth, it is important to evaluate the metabolite composition. Here, the primary metabolism of all the low glycolytic enzymes mutants, PGAM overexpression and complementation lines were analyzed by the GC-MS according to our recently method to provide data set for cross-study comparisons of plant metabolites¹², investigations into the reproducibility of metabolomics data, in-depth analysis of plant metabolism and mathematical modelling of glycolytic flux.

Methods

Plant growth conditions. *Arabidopsis thaliana* genotypes Columbia (Col-0) (WT), *pgk* (SALK_123919), *pgam1-1* (SALK_003321), *pgam 1-2* (SALK_029822), *pgam 2-2* (SALK_002280), *pgam1/2* (SALK_029822/SALK_002280), *enolase2-4* (SAIL_208_E09), *pkc3* (GABI_187A04) and *pkc4* (SALK_143658) mutants, PGAM1 overexpression lines and *pgam1/2* complementation lines (*nA-pgam1/2-1*, (nuclear target PGAM1), *sdmA-pgam1/2-1*, (non-functional PGAM1), *E.pgam-pgam1/2-1* (*E.coli* PGAM), *sdmA-E.pgam-pgam1/2-1* (*E.coli* PGAM and native promoter PGAM1 with nonfunctional PGAM1) and *pgam-pgam1/2* (native PGAM1), Supplementary Table 1) were used in this study. The seeds were plated on Murashige and Skoog medium supplemented with 1% (w/v) sucrose for 10 days, then the seedlings were transferred to soil under 8 h light (22 °C)/16 h dark (18 °C) period (short day) in growth chamber at a light intensity of 120–150 $\mu\text{mol m}^{-2} \text{s}^{-1}$. The PGAM mutant and the overexpression lines were also transferred to 16 h light (22 °C)/8 h dark (18 °C) (long day) in growth chamber at a light intensity of 120–150 $\mu\text{mol m}^{-2} \text{s}^{-1}$ for plant phenotype. The pre-bolting mature rosette leaves of 35-day-old short day *Arabidopsis* were harvested for metabolite measurement after two hours of light (10 am).

Cloning genes of the PGAM. The cytosolically localized PGAM1, PGAM1 with promoter and terminator, *E.coli* PGAM and enolase promoter were amplified and subcloned following previously published protocol¹³. These genes sub-cloned into gateway entry vectors the pDnor207 donor vector by gene specific primers (Supplementary Table 2). The activity site of PGAM1 was mutated by five amino acid (H39, S80, K367, DH470) as primer Supplementary Table 3. Expression vectors for overexpression and complementation were constructed using the Gateway LR reaction with pK7WG2 and PMDC110¹⁴ (Supplementary Table 3).

Plant transformation. These constructs were transformed into the *Agrobacterium tumefaciens* strain GV3101 and then transformed by the floral dip method¹⁵ into wild type plants or the *pgam1/2* double mutant by the green team of the Max Planck Institute of Molecular Plant Physiology. Homozygous overexpression (OE) lines and complementation were selected on MS plates containing 50 mg/L Kanamycin or 100 mg/L Hygromycin. Resistant lines were transferred to soil to grow to maturity, and their transgenic status was confirmed by genomic PCR. Homozygous and complementation T3 seeds of the OE plants were used for further analysis.

Metabolite measurement. Metabolite profiling of *Arabidopsis* leaves was carried out by gas chromatography–mass spectrometry (ChromaTOF software, Pegasus driver 1.61; LECO) as described previously^{16,17}. Briefly, around 50 mg plant materials were frozen and extracted in 700 μl 100% methanol and mixed with 30 μl ribitol (0.2 mg/ml ddH₂O) at room temperature by vortexing. After centrifugation (20000 g, 10 mins), the upper phase was subsequently extracted in 375 μl chloroform and 750 μl ddH₂O. After centrifugation (20000 g, 5 mins) the 150 μl upper phase was dried by speed vac for the GC-MS measurement^{18,19}. Samples were derivatized using the standard protocol¹⁷. Briefly, 40 μl Methoxyaminhydrochlorid (20 mg/ml in Pyridin) was used to resuspend the metabolites with 2 h shaking at 37 °C. 70 μl MSTFA (1 mL MSTFA + 20 μl FAME mix) was added with other 30 mins shark at 37 °C. The supernatant was transferred to GC sample vials. The chromatograms and mass spectra were evaluated using ChromaTOF software. Metabolite identification was manually checked by the mass spectral and retention index collection of the Golm Metabolome Database²⁰. Peak heights of the mass fragments were normalized on the basis of the fresh weight of the sample and the added amount of an internal standard (Ribitol). Statistical differences between groups were analyzed by Student's *t*-tests on the raw data. Results were determined to be statistically different at a probability level of $P < 0.05$. Relative metabolite levels were obtained as the ratio

between the lines and the mean value of the respective wild type (Supplementary Tables 4, 5 and 6). This method is related to our standard protocol¹². Principal component analysis (PCA) was performed using MetaboAnalyst (<https://www.metaboanalyst.ca/>).

Data Records

Raw data of GC-MS have been deposited in the Metabolights²¹ (MTBLS4066²²: Metabolite profiling of Arabidopsis mutants of lower glycolysis) with Arabidopsis wild-type (Col-O), eight mutants, three overexpression and six complementation lines. Raw data contained quality control with 41 metabolites as standard for data analysis. Peg files contain ion detections without data of in-source fragmentation using collision energy. This dataset was composed by two parts of measurement. The first part is the seven glycolytic mutants, three overexpression lines and one wild-type each with six biological replicates. It had 61 metabolites which could be easily characterized (Supplementary Tables 4 and 5, detail analysis at metabolights raw1). The second part is the *ipgam1/2* complementation lines with double mutant and WT with six biological replicates. All the metabolite data were analyzed by the ChromaTOF software and searched on the Golm Metabolome Database as mentioned above. The second part contained 48 well characterized metabolites (Supplementary Table 6, detail analysis at metabolights raw2). The details of the data analysis upload to metabolights as raw1 and raw2.

Technical Validation

The standard deviation was calculated to qualitatively validate metabolite data obtained from at least four biological samples as the square root of variance by determining each data point's deviation relative to the mean. Metabolites were qualitatively validated either by forty-one chemical standards (QC) or by Arabidopsis controls (Supplementary Table 7).

Usage Notes

Plant phenotype and metabolite profiles of *pgk*, phosphoglycerate mutase, phosphoglycerate mutase 2, enolase, *pkc3*, *pkc4* mutants. Given that the phosphoglycerate mutase, enolase and pyruvate kinase complex plays an important role in plant growth, 3PGA metabolism and the chloroplast mitochondria association, both the plant growth phenotype and metabolite profiling analysis were carried out on the respective mutant lines (Fig. 1A). Given that the PGK can also use 3PGA, the mutant of *pgk* was selected and demonstrated to grow more slowly compared with the wild type. The levels of several amino acids and sugars were significantly changed compared with WT plant (Fig. 1B). The plant growth phenotypes of *phosphoglycerate mutase 1* and *phosphoglycerate mutase 2* have been published⁸, but the metabolic changes occurring in these mutant remains unclear. The *phosphoglycerate mutase 1* mutant exhibited decreased contents of glycine and glucose, while *phosphoglycerate mutase 1* mutant significantly decreased several amino acids and fructose and glucose. The *enolase* mutant, however, was characterized by reduced shoot and root growth, altered vascular development and defective secondary growth of stems, impaired floral organogenesis and defective male gametophyte function, resulting in embryo lethality as well as delayed senescence. In our metabolite analysis, the *enolase* mutant contained low amount of amino acids and sucrose, indicating an important role of sucrose synthesis and glycolysis (Fig. 1B and C). The mutant of *pkc3* and *pkc4* neither showed the significant phenotypic changes following growth on 1% glucose medium or on soil. Metabolic profiling of this mutant revealed that galactinol and urea were increased, while mannose, aconitic acid, adipic acid and several amino acids were decreased (Fig. 1B). However, the biological significance of these changes remains unclear.

Plant growth phenotype and metabolite profiles of phosphoglycerate mutase 1 overexpression and mutant. Given the presence of the lower glycolysis metabolon of PGAM, enolase and pyruvate kinase likely plays an important role in the metabolite exchange of chloroplast and mitochondria², phosphoglycerate mutase 1 was overexpressed under the control of the constitutive 35S promoter (Fig. 2). The plant growth phenotype was neither significantly altered in short or long day, while the overexpression lines grew faster in the low light condition with four~six more leaves per plant (Fig. 2A). In the metabolite profiling analysis of normal light condition, the OE lines had lower content of 3PGA, glucose, fructose, arginine, asparagine, glutamine, proline, galactinol and adipic acid (Fig. 2B,C). By contrast, the content of alanine and pyruvate acid were significantly increased in the OE lines.

Complementation of the metabolic and morphological phenotypes. In our former research, the physical interaction between the mitochondria and chloroplast appears to be greatly influenced by the phosphoglycerate mutase-enolase-pyruvate kinase association which we demonstrate above has the capacity to very highly efficiently convert 3PGA to pyruvate. In order to further study the importance of the constituent enzymes in the co-localization of mitochondria and chloroplasts we studied the phosphoglycerate mutase double mutant and various complemented versions of these mutants at the metabolic, morphological and cell biological levels. The mutants could be fully complemented at both the enzyme activity and plant morphology levels following the expression of the corresponding gene under the control of its native promoter^{8,9}. In addition we alternatively attempted to complement the *pgam* double mutant with the full length PGAM targeted to the nucleus, with a site-directed-mutant effecting a residue of the active site of PGAM1 and thus being catalytically inactive^{8,23}, or with the *E. coli* PGAM. In the nuclear sublocalized PGAM1 complementation lines, the enzyme activity could be partially complemented to levels resembling those previously reported for the single *pgam* mutants⁸, by contrast the plant growth and development could not be recovered and the complemented lines still produced less seeds. In addition, the site-directed-mutated Arabidopsis PGAM could neither complement the enzyme activity nor the plant growth and developmental phenotypes¹. The *E. coli* PGAM did not interact with enolase or TPT and could only recover 50% enzyme activity, it also neither complemented seed production nor seed growth¹⁷.

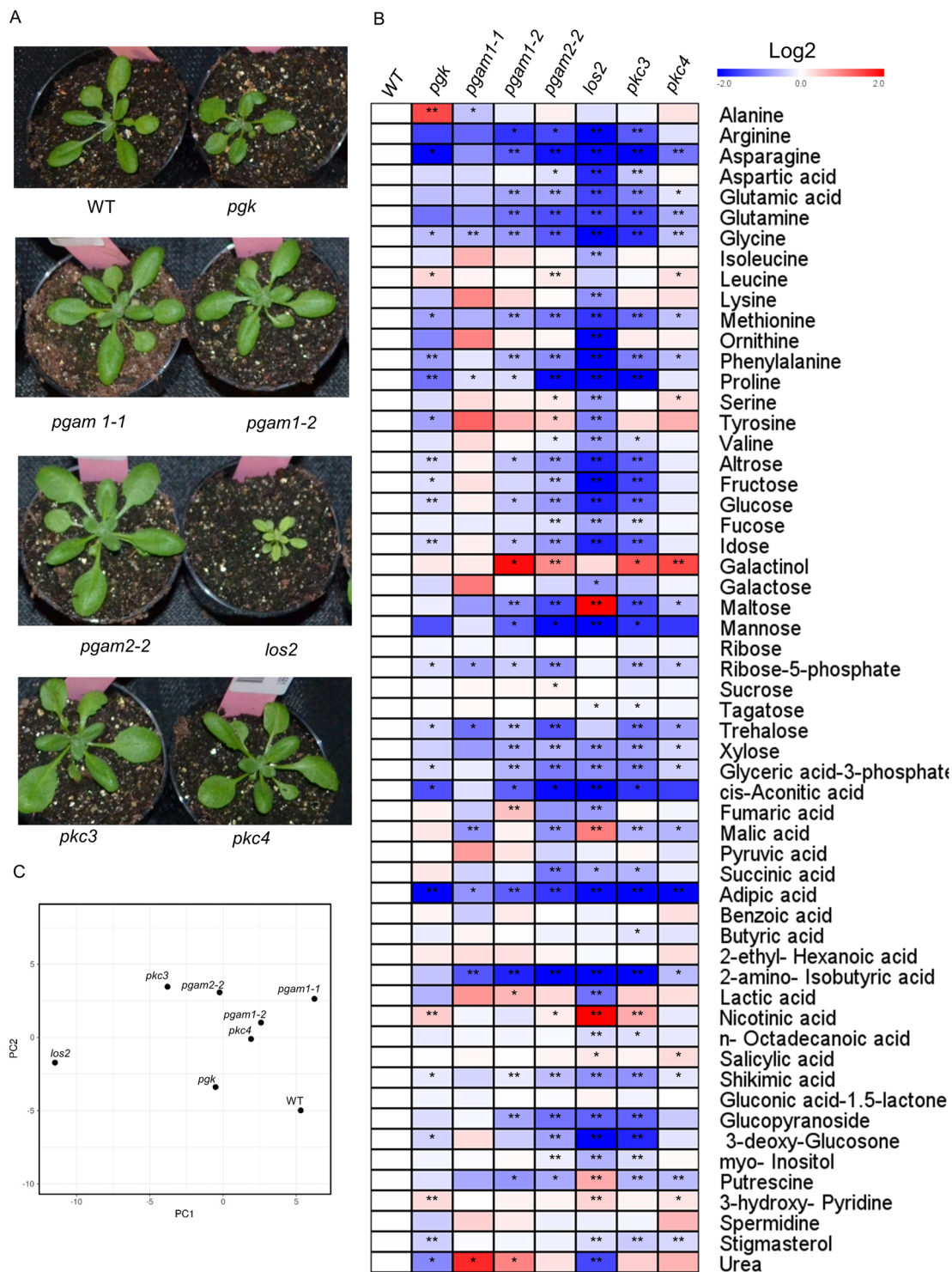


Fig. 1 Plant growth phenotype and metabolite profiling of Arabidopsis mutants. (A) The plant phenotype of 35-day-old plant grew in the green house under short day conditions (8 h light and 16 h dark). Similar to the published growth deficient of enolase⁹, the *pgk* mutant also presented slow growth compared with the wild type, while the other mutant did not show a different growth phenotype. (B) Metabolite profiling of mutants presented as a heat map calculated by log₂ fold change. 30 day-old-plant leaves of SD condition were collected at the 10 am and measured the metabolites by GC-MS (*phosphoglycerate kinase* (*pgk*), *phosphoglycerate mutase 1-1* (*pgam1-1*), *phosphoglycerate mutase 1-2* (*pgam1-2*), *phosphoglycerate mutase 2-2* (*pgam2-2*), *enolase* (*los2*), *pyruvate kinase-3* (*pkc3*) and *pyruvate kinase-4* (*pkc4*)). (C) PCA analyse the metabolism.

Having characterized visible phenotype, we next performed metabolite profiling on the double *pgam* mutants and a number of complementation lines being able to identify 49 primary metabolites using gas chromatography-mass spectrometry (GC-MS) (Fig. 3). In the double mutant, several intermediates of the TCA cycle (fumarate,

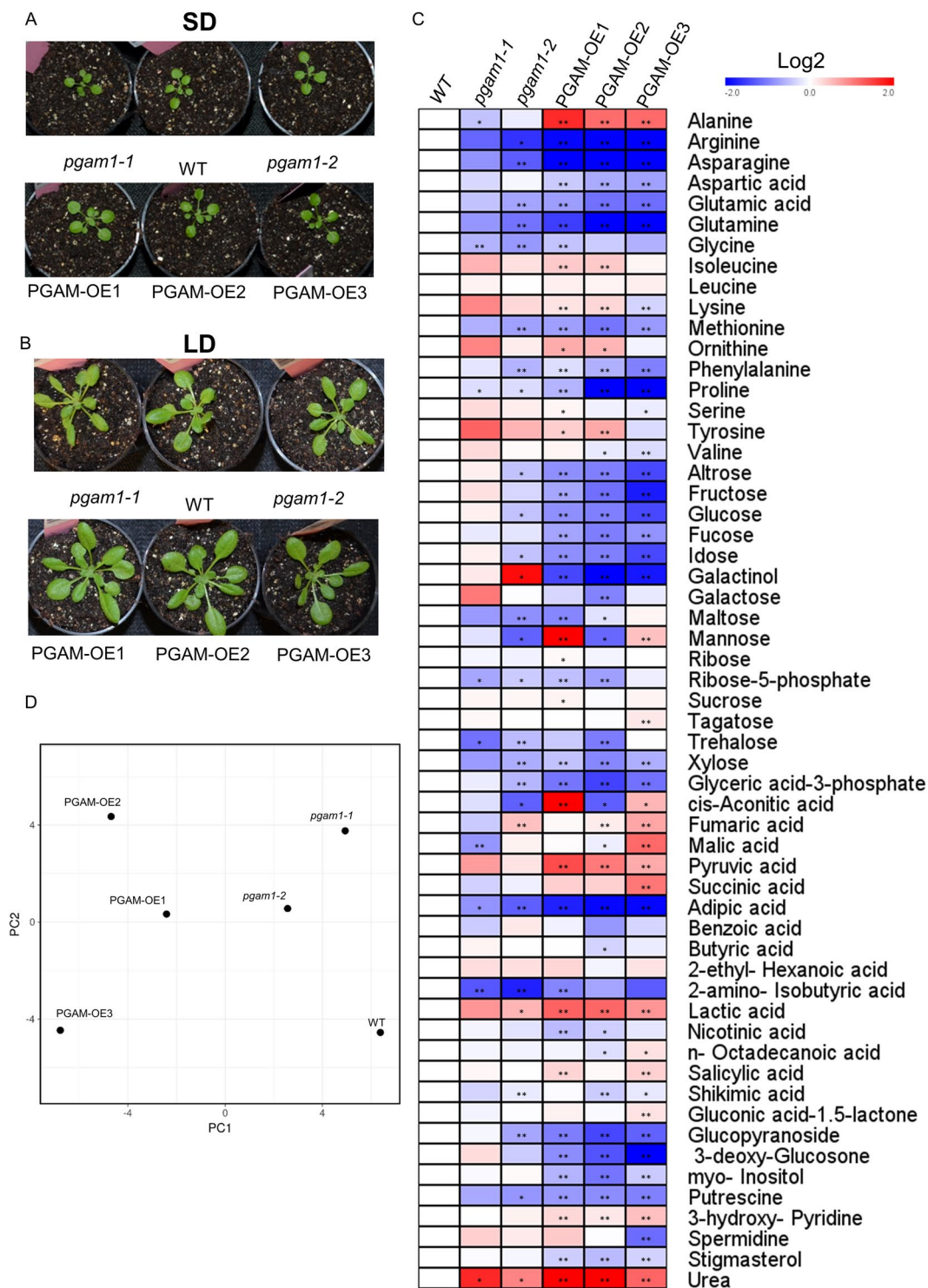


Fig. 2 Plant growth phenotype of and metabolite profiling of PGAM mutant and the overexpression lines. 28 days plants in the short day (SD) (A) and 28 days plants in the long day (LD) condition (B). The phosphoglycerate mutase 1 OE lines grew faster in the LD condition of low light condition while there was no significant difference in the normal condition. (C) Metabolite profiling of mutant and overexpression lines in the heat map calculated by log₂ fold change. 35 days old plant leaves of SD condition were collected at the 10 am and measured the metabolites by GC-MS. (D) PCA analyse the metabolism.

aconitic acid and isocitric acid) and several amino acids (alanine, leucine, phenylalanine and valine) were significantly decreased. However, 3PGA, glycine and serine were increased indicating the importance of the PGAM reaction within the regulation of carbon partitioning. These changes were essentially reverted on the complementation of the PGAM by the expression of PGAM under the control of its native promoter. However, as would

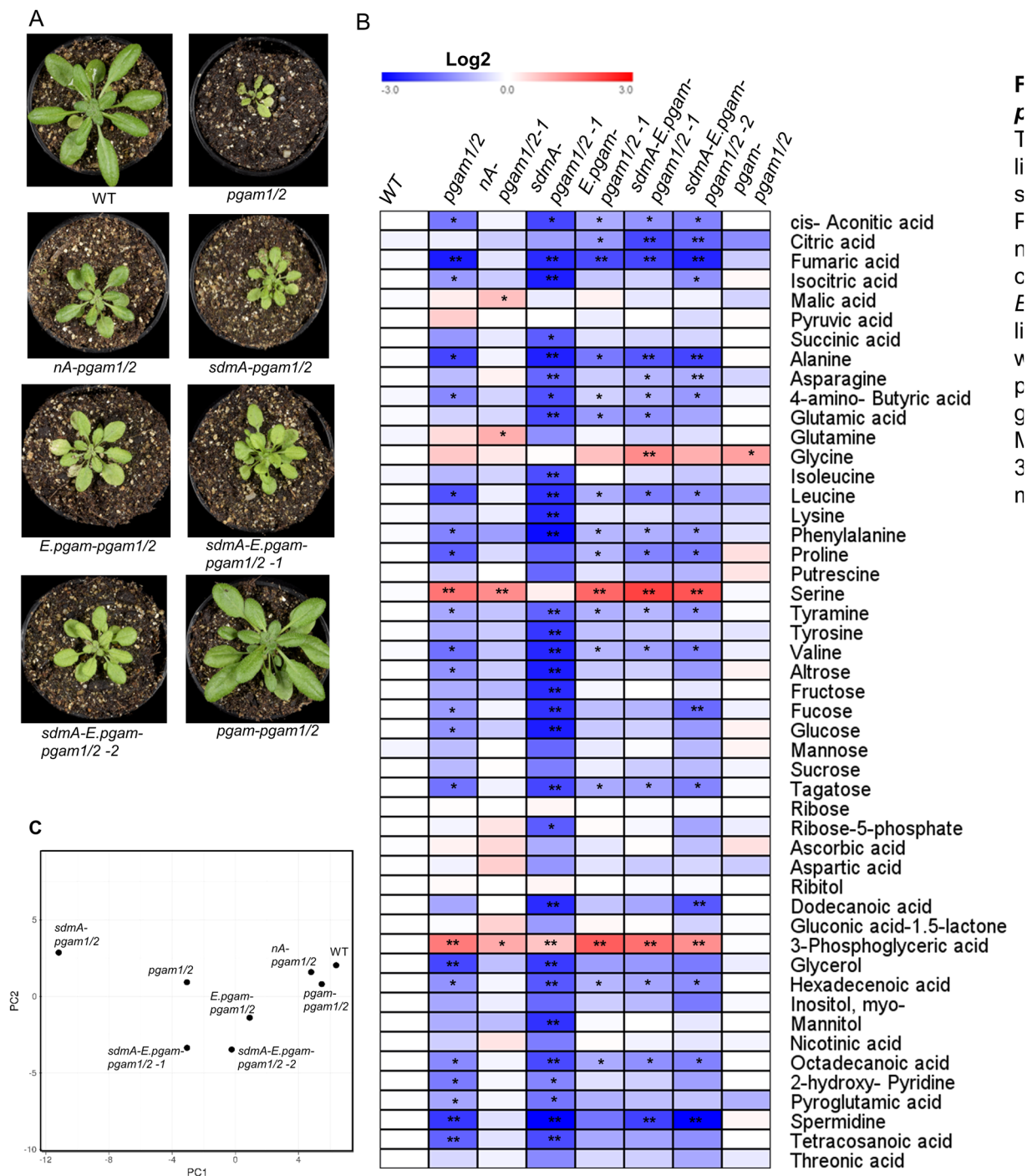


Fig. 3 Plant growth phenotype and metabolite profiling of *phosphoglycerate mutase* double mutant complementation lines and WT. (A) The plant phenotype of 35-day-old plants grown in the greenhouse with short day condition (8 h light and 16 h dark). The double mutant of *phosphoglycerate mutase* is very small in the soil. *nA-pgam1/2-1* and *nA-pgam1/2-2* are two complementation lines native promoter PGAM1 with nuclear target PGAM1. *sdmA-pgam1/2-1* and *sdmA-pgam1/2-2* are two complementation lines native promoter PGAM1 with nonfunctional PGAM1. *E.pgam-pgam1/2-1* and *E.pgam-pgam1/2-2* are two complementation lines native promoter enolase with *E.coli* PGAM. *sdmA-E.pgam-pgam1/2-2* and *sdmA-E.pgam-pgam1/2-2* are two complementation lines native promoter enolase with *E.coli* PGAM and native promoter PGAM1 with nonfunctional PGAM1. *pgam-pgam1/2* is the complementation lines native promoter PGAM1 and full length PGAM1. *nA-enolase-2* is the enolase-2 complemented by native promoter with nuclear target enolase. All the complemented lines presented growth slowly compared with the wild type and full complemented lines. (B) Metabolite profiling presented in the heat map calculated by log2 fold change. 35 days old plant leaves of SD condition were collected at 10 am and measured the metabolites by GC-MS. (C) PCA analysis the metabolism.

perhaps be expected following expression of PGAM in the nucleus had little effect on the metabolome of the double mutant and neither did expression of the catalytically inactive PGAM. Similarly, the ectopic expression of the *E. coli* PGAM under the control of plant enolase native promoter could not complement the mutant metabolome.

Code availability

All code used in this study has been deposited with the data at MetaboLights MTBLS4066²²: Metabolite profiling of Arabidopsis mutants of lower glycolysis.

Received: 23 February 2022; Accepted: 4 September 2022;

Published online: 11 October 2022

References

1. Plaxton, W. C. The organization and regulation of plant glycolysis. *Annual review of plant biology* **47**, 185–214 (1996).
2. Zhang, Y. *et al.* A moonlighting role for enzymes of glycolysis in the co-localization of mitochondria and chloroplasts. *Nature communications* **11**, 1–15 (2020).
3. Flügge, U.-I., Häusler, R. E., Ludewig, F. & Gierth, M. The role of transporters in supplying energy to plant plastids. *Journal of Experimental Botany* **62**, 2381–2392 (2011).
4. Schneider, A. *et al.* An *Arabidopsis thaliana* knock-out mutant of the chloroplast triose phosphate/phosphate translocator is severely compromised only when starch synthesis, but not starch mobilisation is abolished. *Plant Journal* **32**, 685–699 (2002).
5. Hoefnagel, M. H., Atkin, O. K. & Wiskich, J. T. Interdependence between chloroplasts and mitochondria in the light and the dark. *Biochimica et Biophysica Acta (BBA)-Bioenergetics* **1366**, 235–255 (1998).
6. Long, S. P., Marshall-Colon, A. & Zhu, X.-G. Meeting the global food demand of the future by engineering crop photosynthesis and yield potential. *Cell* **161**, 56–66 (2015).
7. Rosa-Téllez, S. *et al.* Phosphoglycerate kinases are co-regulated to adjust metabolism and to optimize growth. *Plant Physiology* **176**, 1182–1198 (2018).
8. Zhao, Z. & Assmann, S. M. The glycolytic enzyme, phosphoglycerate mutase, has critical roles in stomatal movement, vegetative growth, and pollen production in *Arabidopsis thaliana*. *Journal of experimental botany* **62**, 5179–5189 (2011).
9. Eremina, M., Rozhon, W., Yang, S. & Poppenberger, B. ENO 2 activity is required for the development and reproductive success of plants, and is feedback-repressed by A t MBP-1. *The Plant Journal* **81**, 895–906 (2015).
10. Kang, M. *et al.* At MBP-1, an alternative translation product of LOS 2, affects abscisic acid responses and is modulated by the E 3 ubiquitin ligase A t SAP 5. *The Plant Journal* **76**, 481–493 (2013).
11. Wulfert, S., Schilasky, S. & Krueger, S. Transcriptional and Biochemical Characterization of Cytosolic Pyruvate Kinases in *Arabidopsis thaliana*. *Plants* **9**, 353 (2020).
12. Alseekh, S. *et al.* Mass spectrometry-based metabolomics: A guide for annotation, quantification and best reporting practices. *Nature methods* **18**, 747–756 (2021).
13. Zhang, Y. *et al.* Rapid Identification of Protein-Protein Interactions in Plants. *Current protocols in plant biology* **4** (2019).
14. Zhang, Y. J. *et al.* Protein-protein interactions and metabolite channelling in the plant tricarboxylic acid cycle. *Nature Communications* **8** (2017).
15. Clough, S. J. & Bent, A. F. Floral dip: a simplified method for *Agrobacterium*-mediated transformation of *Arabidopsis thaliana*. *Plant Journal* **16**, 735–743 (1998).
16. Lisek, J., Schauer, N., Kopka, J., Willmitzer, L. & Fernie, A. R. Gas chromatography mass spectrometry-based metabolite profiling in plants. *Nature protocols* **1**, 387 (2006).
17. de Souza, L. P., Alseekh, S., Naake, T. & Fernie, A. Mass Spectrometry-Based Untargeted Plant Metabolomics. *Current protocols in plant biology* **4** (2019).
18. Zhang, Y. *et al.* The extra-pathway interactome of the TCA cycle: expected and unexpected metabolic interactions. *Plant Physiol* <https://doi.org/10.1104/pp.17.01687> (2018).
19. Zhang, Y. *et al.* Two mitochondrial phosphatases, PP2c63 and Sal2, are required for posttranslational regulation of the TCA cycle in *Arabidopsis*. *Molecular Plant* **14**, 1104–1118 (2021).
20. Kopka, J. *et al.* GMD@CSB. DB: the Golm metabolome database. *Bioinformatics* **21**, 1635–1638 (2004).
21. Haug, K. *et al.* MetaboLights: a resource evolving in response to the needs of its scientific community. *Nucleic acids research* **48**, D440–D444 (2020).
22. *MetaboLights*, <https://identifiers.org/metabolights:MTBLS4066> (2022).
23. Wang, Y. *et al.* Crystal structure of human B-type phosphoglycerate mutase bound with citrate. *Biochemical and biophysical research communications* **331**, 1207–1215 (2005).

Acknowledgements

A.R.F and Y.J.Z would like to thank the European Union's Horizon 2020 research and innovation programme, project PlantaSYST (SGA-CSA No. 739582 under FPA No. 664620) for supporting their research.

Author contributions

Y.Z. process the metabolites measurement and Y.Z. and A.R.F. wrote the manuscript and both agreed to the published version of the manuscript.

Funding

Open Access funding enabled and organized by Projekt DEAL.

Competing interests

The authors declare no competing interests.

Additional information

Supplementary information The online version contains supplementary material available at <https://doi.org/10.1038/s41597-022-01673-z>.

Correspondence and requests for materials should be addressed to Y.Z. or A.R.F.

Reprints and permissions information is available at www.nature.com/reprints.

Publisher's note Springer Nature remains neutral with regard to jurisdictional claims in published maps and institutional affiliations.



Open Access This article is licensed under a Creative Commons Attribution 4.0 International License, which permits use, sharing, adaptation, distribution and reproduction in any medium or format, as long as you give appropriate credit to the original author(s) and the source, provide a link to the Creative Commons license, and indicate if changes were made. The images or other third party material in this article are included in the article's Creative Commons license, unless indicated otherwise in a credit line to the material. If material is not included in the article's Creative Commons license and your intended use is not permitted by statutory regulation or exceeds the permitted use, you will need to obtain permission directly from the copyright holder. To view a copy of this license, visit <http://creativecommons.org/licenses/by/4.0/>.

© The Author(s) 2022